5-3-2003

Kinetic and Spectroscopic Characterization of the H178A Methionyl Aminopeptidase from *Escherichia coli*

Alicja J. Copik
Utah State University

Sabina I. Swierczek
Utah State University

W. Todd Lowther
University of Oregon

Ventris M. D'Souza
Utah State University

Brian W. Matthews
University of Oregon

See next page for additional authors

Authors

Alicja J. Copik, Sabina I. Swierczek, W. Todd Lowther, Ventris M. D'Souza, Brian W. Matthews, and Richard C. Holz

Kinetic and Spectroscopic Characterization of the H178A Methionyl Aminopeptidase from Escherichia coli

Alicja J. Copik
Sabina I. Swierczek
W. Todd Lowther
Ventris M. D'souza
Brian W. Matthews
Richard C. Holz
Department of Chemistry and Biochemistry, Utah State University, Logan, Utah 84322-0300 and The Howard Hughes Medical Institute, Institute of Molecular Biology, University of Oregon, Eugene, Oregon 97403

Abstract

To gain insight into the role of the strictly conserved histidine residue, H178, in the reaction mechanism of the methionyl aminopeptidase from *Escherichia coli* (*Ec*MetAP-I), the H178A mutant enzyme was prepared. Metal-reconstituted H178A binds only one equivalent of Co(II) or Fe(II) tightly with affinities that are identical to the WT enzyme based on kinetic and isothermal titration calorimetry (ITC) data. Electronic absorption spectra of Co(II)-loaded H178A *Ec*MetAP-I indicate that the active site divalent metal ion is pentacoordinate, identical to the WT enzyme. These data indicate that the metal binding site has not been affected by altering H178. The effect of altering H178 on activity is, in general, due to a decrease

in k_{cat}. The k_{cat} value for Co(II)-loaded H178A decreased 70-fold toward MGMM and 290-fold toward MP-p-NA compared to the WT enzyme, while k_{cat} decreased 50-fold toward MGMM for the Fe(II)-loaded H178A enzyme and 140-fold toward MP-p-NA. The K_m values for MGMM remained unaffected, while those for MP-p-NA increased approximately 2-fold for Co(II)- and Fe(II)-loaded H178A. The k_{cat}/K_m values for both Co(II)- and Fe(II)-loaded H178A toward both substrates ranged from ~50- to 580-fold reduction. The pH dependence of log K_m, log k_{cat}, and log(k_{cat}/K_m) of both WT and H178A EcMetAP-I were also obtained and are identical, within error, for H178A and WT EcMetAP-I. Therefore, H178A is catalytically important but is not required for catalysis. Assignment of one of the observed pK_a values at 8.1 for WT EcMetAP-I was obtained from plots of molar absorptivity at $\lambda_{max(640)}$ vs pH for both WT and H178A EcMetAP-I. Apparent pK_a values of 8.1 and 7.6 were obtained for WT and H178A EcMetAP-I, respectively, and were assigned to the deprotonation of a metal-bound water molecule. The data reported herein provide support for the key elements of the previously proposed mechanism and suggest that a similar mechanism can apply to the enzyme with a single metal in the active site.

Methionyl aminopeptidases (MetAPs)[1]represent a unique class of protease that is capable of removing an N-terminal methionine residue from nascent polypeptide chains (*1−4*). Since the biosynthesis of all prokaryotic and eukaryotic proteins present in the cytosol starts with the initiator methionine, MetAPs play a central role in protein synthesis. While the rationale for the removal of the initiator methionine remains unclear, several explanations have been proposed (*5*). Some involve the facilitation of further processing after excision of the N-terminal groups such as the removal of signal sequences if present, proteolytic cleavage to generate shorter peptides, and the covalent attachment of residues and blocking groups such as acetyl or myristoyl groups (*4*). The structure of mature N-termini play important roles in N-directed degradation pathways and also in targeting of cellular membranes (*6, 7*). MetAPs are therefore one of the key cellular enzymes involved in protein maturation. The physiological importance of MetAP activity is underscored by the lethality upon the deletion of the MetAP gene in *Escherichia coli, Salmonella typhimurium*, and *Saccharomyces cerevisiae* (*8−11*). Moreover, MetAPs have recently been identified as the molecular target for the epoxide-containing anti-angiogenesis agents ovalicin and fumagilin, one of which is in phase III clinical trials (*12−16*). Therefore, MetAPs represent an important target for the development of anti-angiogenesis agents for cancer therapy as well as antibacterial and/or antifungal drugs (*17*).

MetAPs are organized into two classes (types I and II) based on the absence or presence of an extra 62-amino acid sequence (of unknown function) inserted near the catalytic domain. The type-I MetAP from *E. coli* (*Ec*MetAP-I), and the type II MetAPs from *Homo sapiens* (*Hs*MetAP-II) and *Pyrococcus furiosus* (*Pf*MetAP-II) have been crystallographically characterized (*16,18−21*). In all three structures, identical catalytic domains have been observed that contain a bis(μ-carboxylato)(μ-aquo/hydroxo)dicobalt core with an additional carboxylate residue at each metal site and a single histidine bound only to the first metal ion. Recently, it was suggested that the in vivo metal ion for *Ec*MetAP-I is Fe(II), based on a combination of whole cell metal analyses and activity measurements as well as in vitro activity measurements and substrate binding constants (*22, 23*). In addition, the observed catalytic activity as a function of divalent metal ion concentration and the metal binding constants for both Fe(II) and Co(II) *Ec*MetAP-I and *Pf*MetAP-II led to the proposal that MetAPs function as mononuclear enzymes in vivo (*23, 24*). The high-affinity or catalytically relevant metal binding site was assigned as the histidine-containing site by ^{1}H NMR spectroscopy (*23*), which was recently verified by extended X-ray absorption fine structure (EXAFS) spectroscopy (*25*).

A common feature among metalloproteases is an ionizable group within close proximity of the active site that functions as a general acid and/or base (*26−30*). For example, in thermolysin (*26*) and carboxypeptidase A (*30*), a glutamate is considered to play this role by assisting in the deprotonation of the metal bound water molecule. Within the active site of all MetAPs, three solvent molecules exist, the first of which bridges between the two cobalt ions, while a second is terminally ligated to Co2 (*16, 18−21*). A third solvent molecule bridges between an active site histidine residue, H178, and the water molecule that

bridges between the two Co(II) ions. H178 is in close proximity to both cobalt ions (5.1 Å from Co1 and 6.6 Å from Co2), and is strictly conserved among all MetAPs studied to date. Recent crystallographic studies on the transition-state analogue inhibitor, methionine phosphonate (l-MetP) bound to EcMetAP-I, revealed that a phosphonate oxygen atom bridges between Co1 and H178 ([21]). On the basis of these data, the catalytic role of H178 was proposed to be stabilization of the transition state ([20, 31]). Earlier studies on H178A EcMetAP-I showed that the variant has 50-fold lower activity as compared to wild-type EcMetAP-I ([20]). To gain insight into the role of H178 in the catalytic mechanism of N-terminal cleavage of methionine by EcMetAP-I, the H178A EcMetAP-I enzyme has been characterized by kinetic and spectroscopic methods in greater detail and its role in the catalytic mechanism is discussed.

Materials and Methods

Mutagenesis, Protein Expression, and Purification. The H178A altered EcMetAP-I enzyme was generated as previously reported ([15]). The codon encoding the H178A mutation was placed in the wild-type (WT) expression system for EcMetAP-I containing the R175Q mutation (mutation eliminating a secondary thrombin cleavage site) in an analogous manner using the following mutagenic primers: 5'-CGG TTG TTC AGC GAA GCC CTG GCC G-3' and 5'-TGA AGA ACC GCA GGT GCT GCA C-3'. Recombinant WT and H178A EcMetAP-I were expressed and purified as previously described ([22, 23]). Purified H178A EcMetAP-I exhibited a single band on SDS−PAGE and a single symmetrical peak in matrix-assisted laser desorption ionization-time-of-flight (MALDI-TOF) spectrometric analysis indicating $M_r = 29\,630 \pm 10$. Protein concentrations were estimated from the absorbance at 280 nm using an extinction coefficient of 16 450 M^{-1}cm^{-1}. Apo-EcMetAP-I H178A samples were exchanged into 25 mM HEPES, pH 7.5, containing 150 mM KCl (Centricon-10, Millipore Corp).

Metal Content Measurements. The H178A EcMetAP-I and wild-type control samples used for metal analysis were typically 30 μM. Apo-EcMetAP-I samples were incubated under anaerobic conditions with MCl$_2$, where M = Co(II) or Fe(II) (MCl$_2$: ≥ 99.999% Strem Chemicals, Newburyport, MA or Aldrich) for 30 min. prior to exhaustive dialysis under anaerobic conditions against Chelex-treated buffer as previously reported ([22, 23]). Analyses were performed using inductively coupled plasma-atomic emission spectrometry (ICP-AES).

Enzymatic Assay of H178A EcMetAP-I. H178A EcMetAP-I was assayed for catalytic activity with the tetrapeptide MGMM as the substrate (8 mM) using an HPLC method as previously described ([23]). This method is based on the spectrophotometric quantitation of the reaction product GMM following separation on a C8 HPLC column (Phenomenex, Luna; 5μ, 4.6 × 25 cm). The kinetic parameter v (velocity) was determined at pH 7.5 by quantifying the tripeptide GMM at 215 nm in triplicate. One unit of activity is defined as the amount of enzyme that produces one micromole of GMM in one minute. The hydrolysis of MP-p-NA was monitored spectrophotometrically at 405 nm based on the increase in absorbance of p-NA ($\Delta\varepsilon_{405}$ value of p-nitroaniline of 10 600 M^{-1} cm^{-1}) using a coupled assay ([32]). The reaction mixture consisted of a 5 μL aliquot of a 10 μM enzyme solution, 3 μL of a 2.0 mM prolidase in 20 mM Tris containing 30% glycerol. Various concentrations of substrate were added to the enzyme solution to a final volume of 1000 μL (25 mM HEPES in chelexed water at pH 7.5 containing 150 mM KCl). Enzyme activities are expressed as units/mg, where one unit is defined as the amount of enzyme that releases one micromole of product at 30 °C in one minute. Catalytic activities were determined with an error of ± 10%.

Isothermal Titration Calorimetry. Isothermal titration calorimetry (ITC) measurements were carried out on a MicroCal OMEGA ultrasensitive titration calorimeter. The titrant (CoCl$_2$) and apo-EcMetAP-I solutions of WT and H178A were prepared in chelexed 25 mM HEPES buffer at pH 7.5, containing 150 mM KCl. Stock buffer solutions were thoroughly degassed before each titration. The enzyme solution (70 μM) was placed in the calorimeter cell and stirred at 200 rpm to ensure rapid mixing. Typically, 3 μL of titrant was delivered over 7.6 s with a 5-min interval between injections to allow for complete equilibration. Each titration was continued until 4.5−6 equiv of Co(II) had been added to ensure that no additional complexes were formed in excess titrant. A background titration, consisting of the identical titrant solution but only

the buffer solution in the sample cell, was subtracted from each experimental titration to account for heat of dilution. The data were analyzed with a two- or three-site binding model by the Windows-based Origin software package supplied by MicroCal.

pH Studies. The enzymatic activity of WT and H178A *Ec*MetAP-I enzymes were measured using MGMM as the substrate. Apo-enzyme samples were incubated with Co(II) at 30 °C for 30 min prior to reaction to ensure metal binding. The enzyme concentration used in the reaction mixture was 2 μM for WT and 6 μM for H178A *Ec*MetAP-I. The reaction time was 1 min for the WT enzyme and 1 h for H178A *Ec*MetAP-I. All buffers were 30 mM with 150 mM KCl. The buffers used were as follows: pH 5.5−6.0, MES; pH 6.5−6.75, PIPES; pH 7.0−8.0 HEPES; pH 8.0−8.5 EPPS. The kinetic parameters k_{cat}, K_m, and k_{cat}/K_m, were determined using 10−12 different substrate concentrations (0−16 mM) at each pH value and these data were fit to the Michaelis−Menten equation by nonlinear least-squares methods using IGOR Pro. The enzyme stability at each pH studied was examined by incubating the enzyme at the desired pH for the assay time (time of incubation with metal plus reaction) followed by adjustment of the pH back to pH 7.5 by a 100-fold dilution with HEPES buffer (pH 7.5, 150 mM KCl) after which the pH was reexamined and the specific activity determined.

Spectroscopic Measurements. Electronic absorption spectra were recorded on a Shimadzu UV-3101PC spectrophotometer. All apo-*Ec*MetAP-I samples used in spectroscopic measurements were rigorously anaerobic prior to incubation with Co(II) (CoCl$_2$) for ~20 min at 25 °C. Co(II)-containing samples were handled throughout in an anaerobic glovebox (N$_2$/5% H$_2$, ≤ 1 ppm O$_2$; Coy Laboratories). Electronic absorption spectra were normalized for protein concentration and the absorption due to uncomplexed Co(II) ($\varepsilon_{512\ nm}$ = 6.0 M^{-1} cm^{-1}). UV−Vis spectra recorded at different pH values contained enzyme that had been exchanged into the appropriate buffer at the desired pH and incubated with one equivalent of Co(II) at 4 °C.

Results

Metal Content and Specific Activity of H178A EcMetAP-I. The number of tightly bound divalent metal ions was determined for H178A *Ec*MetAP-I by ICP-AES analysis. Apo-enzyme samples (30 μM), to which 2−30 equiv of Co(II) or Fe(II) were added under anaerobic conditions, were dialyzed extensively at 4 °C with chelexed, metal-free HEPES buffer (25 mM HEPES, 150 mM KCl, pH 7.5). ICP-AES analysis revealed 1.0 ± 0.1 equiv of cobalt or iron associated with the H178A *Ec*MetAP-I enzyme. These data suggest that only one divalent metal ion is tightly bound to the H178A mutant enzyme, while the second metal ion is labile on the time scale of the buffer exchange (3 h, 4 °C).

The specific activity of the H178A *Ec*MetAP-I was examined with MGMM and MP-*p*-NA as substrates. Kinetic parameters were determined for both Co(II) and Fe(II) reconstituted WT and H178A enzymes (Table 1). The effect on activity after mutating H178 to alanine is in general due to a decrease in k_{cat}. The k_{cat} value for Co(II)-loaded H178A decreased 70-fold toward MGMM and 290-fold toward MP-*p*-NA compared to the WT enzyme, while k_{cat} decreased 50-fold toward MGMM for the Fe(II)-loaded H178A enzyme and 140-fold toward MP-*p*-NA. The K_m values for MGMM remained unaffected, while those for MP-*p*-NA increased approximately 2-fold for Co(II)- and Fe(II)-loaded H178A (Table 1). The k_{cat}/K_m values for Co(II)-loaded H178A toward MGMM and MP-*p*-NA decreased 50 and 580-fold, respectively. Similarly, k_{cat}/K_m values for Fe(II)-loaded H178A toward MGMM and MP-*p*-NA decreased 50- and 200-fold, respectively.

Table 1: Kinetic Parameters for Hydrolysis of MGMM and MP*p*NA by Co(II) and Fe(II) Loaded *Ec*MetAP-I[a]

		MGMM		MP-*p*-NA	
	substrate	wild-type	H178A	wild-type	H178A
Co(II)	K_m (mM)	3.2 ± 0.1	3.2 ± 0.2	0.06 ± 0.01	0.12 ± 0.02
	V_{max} (U/mg)	77 ± 3	1.1 ± 0.1	1.2 ± 0.2	0.004 ± 0.002
	k_{cat} (s^{-1})	39	0.54	0.59	0.002

	k_{cat}/K_m (M⁻¹s⁻¹)	12200	170	9800	15
Fe(II)	K_m(mM)	2.0 ± 0.3	2.0 ± 0.3	0.09 ± 0.01	0.13 ± 0.02
	V_{max} (U/mg)	55 ± 3	1.2 ± 0.1	2.9 ± 0.3	0.02 ± 0.005
	k_{cat} (s⁻¹)	28	0.56	1.4	0.01
	k_{cat}/K_m (M⁻¹s⁻¹)	14000	280	16800	85

[a] Activity assays were performed in 25 mM HEPES, pH 7.5, 150 mM KCl with 12 μM $CoCl_2$ or $Fe(SO_4)$.

Fe(II) Metal Binding Constant for H178A EcMetAP-I. The extent of hydrolytic activity exhibited by the H178A *Ec*MetAP-I enzyme was determined as a function of Fe(II) concentration (Figure 1). The H178A apo-*Ec*MetAP-I enzyme was incubated for 30 min under anaerobic conditions at pH 7.5 with varying amounts of Fe(II) and the level of catalytic activity was determined. Upon the addition of Fe(II) to H178A *Ec*MetAP-I, the specific activity increased as a function of metal ion concentration and exhibited a maximum activity of ~1.1 units mg⁻¹ after the addition of only one equivalent of Fe(II). Further additions resulted in little change in the observed level of activity and above four equivalents of Fe(II), the enzymatic activity decreased. These data are identical to those observed for Fe(II) binding to WT *Ec*MetAP-I ([22, 23]). The activity titration data for Fe(II) binding to the H178A *Ec*MetAP were fit to eq 1 (Figure 1) ([33]):

$$r = pC_s/(K_d + C_s) \ (1)$$

where p is the number of sites for which interaction with ligand is governed by the intrinsic dissociation constant K_d, C_s is the free metal concentration (Fe_{free} in this case), and r is the binding function which was calculated by conversion of the fractional saturation ($r = f_a p$) as previously described ([23]). Free metal concentration was calculated from

$$C_S = C_{TS} + rC_A \ (2)$$

where C_{TS} and C_A are the total molar concentrations of metal and enzyme, respectively. The best fit obtained exhibited a p value of 1 and a K_d value of 0.30 ± 0.15 μM (Figure 1). These data are identical, within error, to those obtained for Fe(II) binding to WT *Ec*MetAP-I ($K_d = 0.20 ± 0.15$ μM) ([23]).
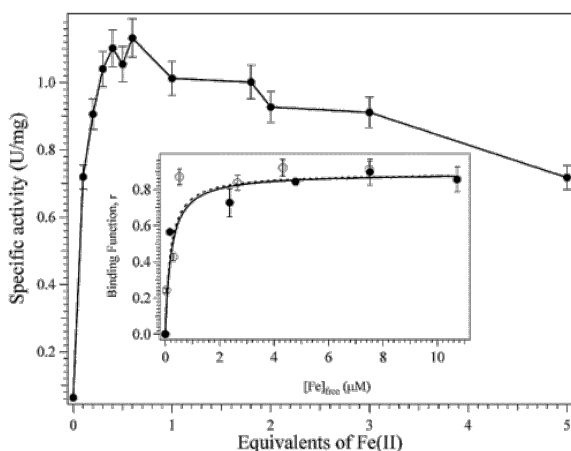

Figure 1 Plot of specific activity (U/mg) of H178A *Ec*MetAP-I vs equivalents of Fe(II). Activity assays were performed with 8 mM MGMM in 25 mM HEPES, pH 7.5, 150 mM KCl. Inset: Plot of binding function, r, vs free Fe(II) concentration, Fe(II)$_{free}$, for WT *Ec*MetAP-I (○) and H178A *Ec*MetAP-I (·). The solid line represents a fit of Fe(II) activity titration data for H178A *Ec*MetAP-I to eq 1. This fit provided a value of $p = 1$ and a K_d value of 0.30 ± 0.15 μM (Figure 1). These data are identical, within error, to those obtained for Fe(II) binding to WT *Ec*MetAP-I (dashed line, $K_d = 0.20 ± 0.15$ μM).

Isothermal Titration Calorimetry. Isothermal titration calorimetry (ITC) measurements were carried out at 20 ± 0.2 °C for both WT and H178A *Ec*MetAP-I (Figure 2A,C). Association constants (K_b) were obtained by

fitting these data, after subtraction of the background heat of dilution, via an iterative process using the Origin software package. This software package uses a nonlinear least-squares algorithm that allows the concentrations of the titrant and the sample to be fit to the heat-flow-per-injection to an equilibrium binding equation for two sets of noninteracting sites. The K_b value, the metal-enzyme stoichiometry (n), and the change in enthalpy (ΔH^o) were allowed to vary during the fitting process (Table 2, Figure 2B,D). The best fits obtained for both WT and altered EcMetAP-I provided an overall n value of 3 for three noninteracting sites. Attempts to fit these data with n values of 1 or 2 provided poor fits, as did fits in which the n value was 3 but the binding process was considered cooperative. For WT EcMetAP-I, a K_d value of 6.4 $\pm$ 0.5 μM was observed as well as two K_d values of 14 $\pm$ 5 mM. On the other hand, a K_d value of 12.5 $\pm$ 0.5 μM and two K_d values of 29 $\pm$ 5 mM were obtained for H178A. These data correspond to individual binding events of three Co(II) ions to the EcMetAP-I WT and H178A altered enzyme.
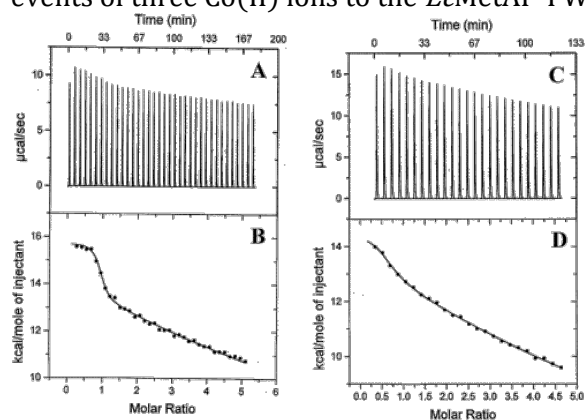

Figure 2 (A) ITC titration of a 70 μM solution of WT EcMetAP-I with a 5 mM Co(II) solution. (C) ITC titration of a 70 μM solution of H178A EcMetAP-I with a 5 mM Co(II) solution. (B) Fit of the ITC data for WT EcMetAP-I and (D) for H178A EcMetAP-I after subtraction of the heat of dilution. The fits were obtained using noninteracting sites model and provided an overall n value of 3, with one tight and two loose sites. Reaction conditions: 20 °C in 25 mM HEPES, pH 7.5, and 150 mM KCl.

Table 2: Dissociation Constants (K_d) and Metal−Enzyme Stoichiometry (n) for Co(II) Binding to Wild-Type and H178A EcMetAP-I[a]

EcMetAP-1	n	K_d1, K_d2 (μM)
	1	6.4 $\pm$ 0.5
wild-type	2	14000 $\pm$ 5000
	1	12.5 $\pm$ 0.5
H178A	2	29000 $\pm$ 5000

[a] For each set of data for both WT and H178A EcMetAP-I, n is the number of Co(II) ions per protein. Data for $n = 1$ are for one Co(II) ion that bound tightly, and data for $n = 2$ represent two Co(II) ions binding to sites on protein with lower affinity.

pH Dependence of Kinetic Parameters of WT and H178A EcMetAP-I. The pH dependence of K_m and V_{max} for WT and H178A EcMetAP-I was examined using MGMM as the substrate (Figure 3). Both WT and H178A EcMetAP-I displayed optimum catalytic efficiency and maximal activity between pH 7.2 and 7.8. The stability of both enzymes at each pH value studied was also examined by incubating the enzyme at the desired pH for the assay time (30 min for WT vs 90 min for H178A EcMetAP-I) followed by adjustment of the pH back to 7.5 after which the specific activity was determined at 8 mM MGMM. For WT EcMetAP-I, full enzymatic activity was recovered up to pH 8.25 above which the recoverable activity decreased by 15% or greater. On the other hand, the amount of recoverable activity for the H178A altered EcMetAP-I enzyme decreased rapidly at pH values greater than ~7.8, indicating a loss of stability under these conditions. For both log(k_{cat}) and log(k_{cat}/K_m), the data obtained above pH 8.0 were corrected for the % loss in activity by eq 3

corrected activity $=$ (experimental activity)$(1/\%$ initial activity) (3)

by normalizing for the activity recoveredafter returning to a standard pH (Figure 3B). This could be done only for the wild-type enzyme because of the short reaction time as compared to total assay time during which the enzyme was exposed to high pH.
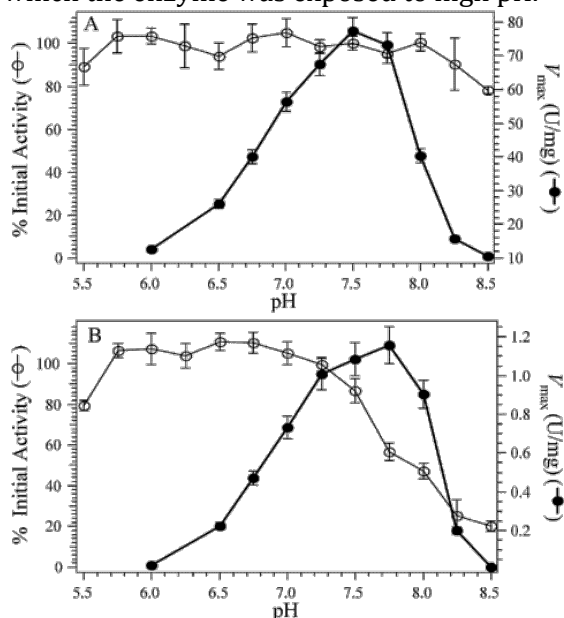

Figure 3 (A) Plot of V_{max} vs pH for WT EcMetAP-I ($\cdot$) and a percent of activity recovered after incubating the enzyme at the desired pH for the assay time (30 min + one minute) followed by adjustment of the pH back to 7.5 after which the specific activity was determined ($\circ$). (B) Plot of V_{max}vs pH for H178A EcMetAP-I ($\cdot$) and a percent of activity recovered after incubating the enzyme at the desired pH for the assay time (30 min + 1 h) followed by adjustment of the pH back to 7.5 after which the specific activity was determined ($\circ$). The assays were performed using 8 mM MGMM as substrate. The Co(II) concentration in the assay was 12 µM.

Plots of $\log(k_{cat})$ and $\log(k_{cat}/K_m)$ vs pH were prepared for both WT and H178A EcMetAP-I and fit to eqs 4 and 5, respectively (Figures 4 and 5) ($34, 35$):

$$\log(k_{cat}) = \log[k'_{cat}/(1 + [H]/K_{ES1} + K_{ES2}/[H])] \ (4)$$

$$\log(/K_m) = \log[(k'_{cat}/K'_m)/(1 + [H]/K_{E1} + K_{E2}/[H])] \ (5)$$

Where k_{cat} is the theoretical maximal velocity, k_{cat}/K'_m is the theoretical maximal catalytic efficiency, K_{ES1} is the ionization constant of the ES complex which affects the acidic side of the pH curve, K_{ES2} reflects the basic side, and K_{E1} and K_{E2} are ionization constants for an acidic and basic group, respectively, on the free enzyme or free substrate (Scheme 1). For the pH dependence of log K_m of WT EcMetAP-I a graphical method was used to determine the pK values (36). There are at least two ionizations present with pK's of 7.5 and 7.9, and the slope of the asymptote is 1 (Figure 4A, Table 3).
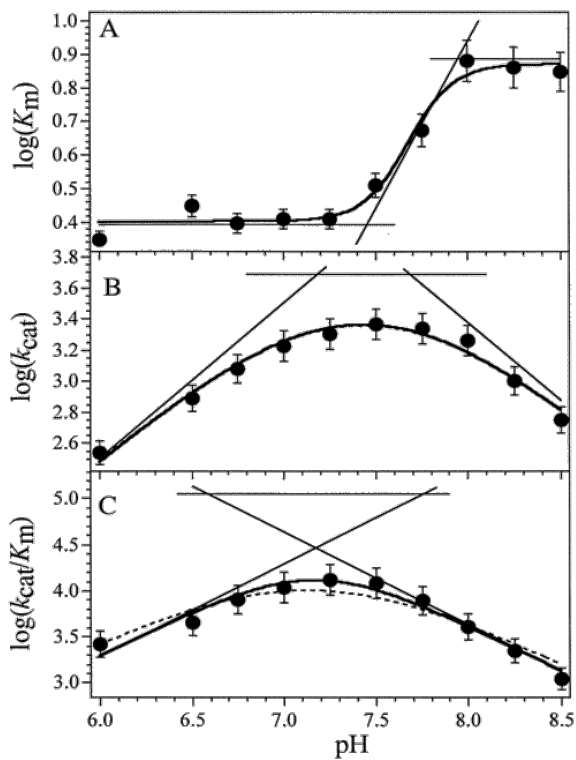
Figure 4 pH dependence of the kinetic parameters for the hydrolysis of MGMM by WT EcMetAP-I between pH 6.0 and 8.5. Data were fitted to eqs 4 and 5 (solid line) plots B and C, respectively. The same data were also fit to eq 10 and 11 (dashed line). (A) $\log(K_m)$ vs. pH. The values $pK_a = 7.5 \pm 0.1$ and 7.9 ± 0.1 were obtained using graphical method. The solid line represents a fit to equation describing a sigmoidal curve and was not used for calculations. (B) $\log(k_{cat})$ vs pH {$pK_{ES1} = 7.2 \pm 0.1$ and $pK_{ES2} = 7.7 \pm 0.1$, $k'_{cat} = (5 \pm 1) \times 10^3$}. (C) $\log(k_{cat}/K_m)$ vs pH {$pK_{E1} = 7.7 \pm 0.5$ and $pK_{E2} = 6.6 \pm 0.5$, $\tilde{k}_{cat}/\tilde{K}_m = (1.1 \pm 0.2) \times 10^5$)}.
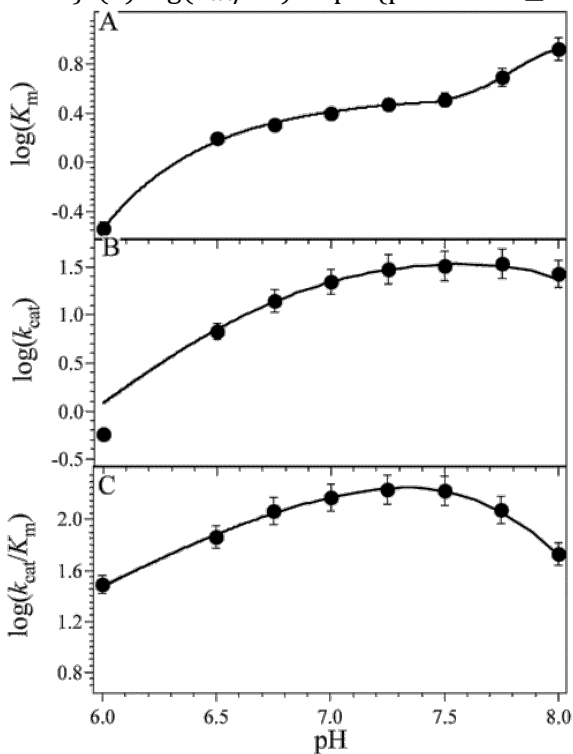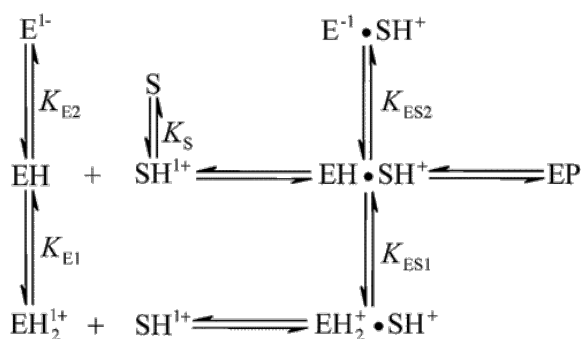

Figure 5 pH dependence of the kinetic parameters for the hydrolysis of MGMM by H178A EcMetAP-I between pH 6.0 and 8.0. (A) $\log(K_m)$ vs pH. (B) $\log(k_{cat})$ vs pH. (C) $\log(k_{cat}/K_m)$ vs pH.

E^{1-} E^{-1}•SH$^+$

K_{E2} S K_{ES2}

     K_S

EH + SH^{1+} ⇌ EH•SH$^+$ ⇌ EP

K_{E1} K_{ES1}

EH$_2^{1+}$ + SH^{1+} ⇌ EH$_2^+$•SH$^+$

Scheme 1 [a]

[a] Molecular dissociation constants are represented by K_{E1} and K_{E2} for the free enzyme, by K_S for the free substrate, and K_{ES1} and K_{ES2} represent those for the enzyme−substrate complex.

Table 3: Ionization Constants for WTEcMetAP-I [a]

K_m vs pH		
pK_1	7.5 ± 0.1	
pK_2	7.9 ± 0.1	
k_{cat} vs pH	equation 4	equation 10
pK_{ES1}	7.2 ± 0.1	7.4 ± 0.3
pK_{ES2}	7.7 ± 0.1	7.4 ± 0.3
k'_{cat}	$(5 ± 1) × 10^3$	$(9 ± 2) × 10^3$
k_{cat}/K_m vs pH	equation 5	equation 11
pK_{E1}	7.7 ± 0.5	7.1 ± 1
pK_{E2}	6.6 ± 0.6	7.1 ± 1
k'_{cat}/K'_m	$(1.1 ± 0.2) × 10^5$	$(4.0 ± 0.1) × 10^5$

[a] For the pH dependence of log(K_m) of WTEcMetAP-I, a graphical method was used to determine the pK values ([36]). Plots of log(k_{cat}) and log(k_{cat}/K_m) vs pH were fit to eqs 4 and 5, respectively. Since the obtained pK_a values differed by less than 0.6 unit the data were also fit to eqs 10 and 11, which are recommended in such cases ([39]).

A plot of log(k_{cat}) vs. pH is a bell-shaped curve that was fit to eq 4 (Figure 4B). A good fit was obtained, which yielded pK_{ES1} of 7.2 ± 0.1 and pK_{ES2} of 7.7 ± 0.1 and $k'_{cat} = (5 ± 1.0) × 10^3$ min^{-1} (Table 3). In addition, fits of log(k_{cat}/K_m) vs pH to eq 5 provided p$K_{E1} = 7.7 ± 0.5$, p$K_{E2} = 6.6 ± 0.6$, and $k'_{cat}/k'_m = (1.1 ± 0.2) × 10^5$ M^{-1} s^{-1}. Since pK_{E2} is less than pK_{E1}, this suggests positive cooperativity for proton binding. The low and high pH asymptotes for plots of log k_{cat} vs pH were calculated using eqs 6 and 7, while low and high pH asymptotes for log(k_{cat}/K_m) vs pH were obtained using eqs 8 and 9 ([37]).

$$\log(y) = \log(k'_{cat}) + \text{pH} - pK_{ES1} \quad (6)$$

$$\log(y) = \log(k'_{cat}) + \text{pH} - pK_{ES2} \quad (7)$$

$$\log(y) = \log(k'_{cat}/k'_m) + \text{pH} - pK_{E1} \quad (8)$$

$$\log(y) = \log(k'_{cat}/k'_m) + \text{pH} - pK_{E2} \quad (9)$$

The asymptotes for k_{cat} have slopes of 1.0 and −1.0 and cross the k'_{cat} at pK_{ES1} and pK_{ES2} (Figure 4B). The asymptotes for plots of log(k_{cat}/K_m) have slopes of 1.0 and −1.0 and exhibit crossover points at the theoretical maximal catalytic efficiency which gives the pK_{E1} and pK_{E2} values (Figure 4C). The two pK's are separated by less than 2 pH units and the observed apparent k_{cat} is below k'_{cat}. In this case, the crossover point of the observed apparent k_{cat} with the asymptotes on the pH curve do not provide pK's ([34, 37, 38]).

The determination of pK_{ES1} and pK_{ES2} becomes inaccurate when pK_{ES2} falls below pK_{ES1} (i.e., when there is strongly cooperative proton binding). The reason for this is that the width of the curve at half its maximal height becomes insensitive to changes in the difference between pK_{ES2} and pK_{ES1} and when $pK_{ES1} > pK_{ES2}$ (_38_). For such cases, eqs 10 and 11 are required (_39_). Fits of $\log(k_{cat})$ vs. pH to eq 10 provided $pK_{ES1} = 7.4 \pm 0.3$, $pK_{ES2} = 7.4 \pm 0.3$ and $k'_{cat} = (9 \pm 2) \times 10^3$ min^{-1}. Fits of $\log(k_{cat}/K_m)$ vs. pH to eq 11 provided $pK_{E1} = 7.1 \pm 1$, $pK_{E2} = 7.1 \pm 1$ and $k'_{cat}/k'_m = (4.0 \pm 0.1) \times 10^5$ M^{-1} s^{-1}.

$$\log(k'_{cat}) = \log\{k'_{cat}/[(1 + [H]/K_{ES1})(1 + K_{ES2}/[H])]\} \ (10)$$

$$\log(k'_{cat}/K_m) = \log\{(k'_{cat}/K'_m)/[(1 + [H]/K_{E1})(1 + K_{E2}/[H])]\} \ (11)$$

Attempts were made to fit the pH-dependent data for H178A _Ec_MetAP-I to the equations described above but failed to yield reasonable pK values (Figure 5). Yet, some qualitative descriptions of the pH-dependent $\log(K_m)$, $\log(k_{cat})$, $\log(k_{cat}/K_m)$ can be made in comparison to the WT data. Plots of $\log(k_{cat})$ or $\log(k_{cat}/K_m)$ vs pH likely form a bell-shaped curve, but this assertion cannot be made conclusively due to the lack of data points above pH 8.0. The acidic limbs of the curves for $\log(k_{cat})$ vs pH (Figure 5B) and $\log(k_{cat}/K_m)$ vs pH (Figure 5C) have slopes near 1 and increase with increasing pH up to pH 7.8 and 7.3, respectively. pK values are not presented due to the lack of data above pH 7.8.

pH Dependence of the Electronic Absorption Spectra of the Co(II)-Substituted WT and H178A EcMetAP-I Enzymes. Electronic absorption spectra of the Co(II)-substituted forms of the WT and H178A _Ec_MetAP-I enzymes were recorded at several pH values between 6.0 and 9.0. At a pH value of 7.5, the electronic absorption spectrum of WT _Ec_MetAP-I with one equivalence of Co(II) contains three absorption maxima at 570 nm ($\varepsilon = 130$ M^{-1} cm^{-1}), 640 nm ($\varepsilon = 135$ M^{-1} cm^{-1}), and 690 nm ($\varepsilon = 105$ M^{-1} cm^{-1}) that can be attributed to Co(II) d−d transitions (Figure 6). The coordination number of the active site Co(II) ion in _Ec_MetAP-I at pH 7.5 is five. However, increasing the pH to 9.0 increases the molar absorptivity at λ_{max} 640 nm from 135 to 290 M^{-1} cm^{-1} while decreasing the pH from 7.5 to 6.5 decreases the molar absorptivity from 135 to 50 M^{-1} cm^{-1} (Figure 6). Interestingly, a similar trend is observed for H178A _Ec_MetAP-I, except that the spectra with similar molar absorptivities to the WT enzyme occur at pH values 0.5 pH units more acidic. A plot of molar absorptivity (ε) of the λ_{max} value at 640 nm vs pH provides simple sigmoidal curves for both WT and H178A _Ec_MetAP-I (Figure 7). These data were fit to eq 12

$$\varepsilon = \varepsilon_{min} + \varepsilon_{max}/[1 + \exp\{(pK_a - pH)/slope\}] \ (12)$$

which gave apparent pK_a values of 8.1 ± 0.5 and 7.6 ± 0.3 for WT and H178A _Ec_MetAP-I, respectively.
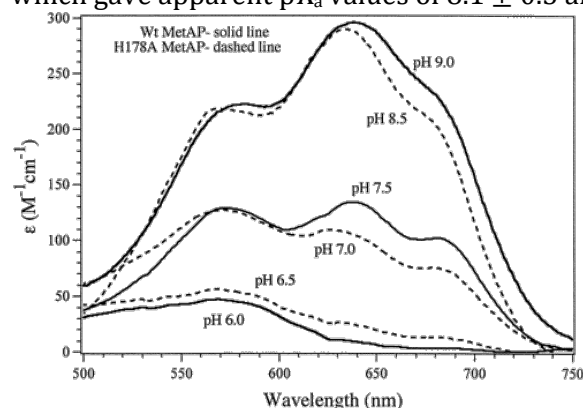

Figure 6 Electronic absorption spectra of Co(II)-loaded WT (solid line) and H178A (dashed line) _Ec_MetAP-I. Visible spectra were recorded at various pH for 1 mM WT and H178A EcMetAP with one equivalence of Co(II).
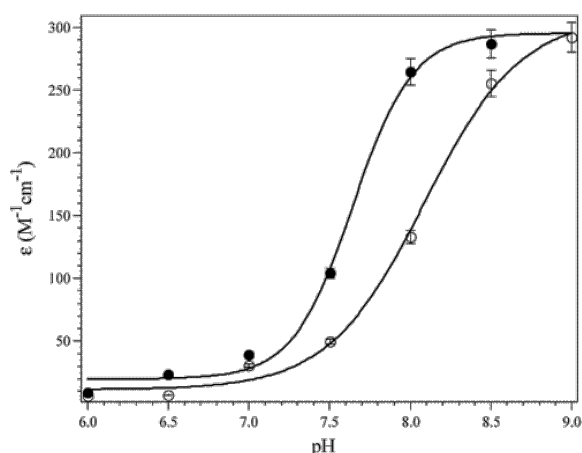
Figure 7 Plots of extinction coefficient (ε) at 640 nm vs pH for wild type (○) and H178A (·) *Ec*MetAP-I. The solid lines represent a fit to an equation of a sigmoidal curve. The midpoints of each curve provided pK_a values 8.0 and 7.6 for WT and H178A *Ec*MetAP-I, respectively.

Discussion

Histidine-178 is strictly conserved in all MetAPs sequenced to date, and it has been suggested that the imidazole of H178 plays a role in the catalytic removal of N-terminal methionine residues from polypeptide chains by MetAPs (*20*, *21*, *31*). Previously, it was shown that the H178A *Ec*MetAP-I altered enzyme exhibited 50-fold lower activity toward norleucine−Ala−Ala−Glu−Glu (Nle-AAEE) in comparison to WT enzyme (*20*). On the basis of these data, it was suggested that H178, while important for catalysis, was not a catalytically required residue. To more clearly define the role of H178 in catalysis, we have examined the H178A altered *Ec*MetAP-I enzyme and found that the amount of catalytic activity retained (~1.5%) is dependent on both the substrate and the divalent metal ion present.

The specific activity of H178A altered *Ec*MetAP-I enzyme was determined in the presence of both the tetrapeptide MGMM and the *para*-nitroanilide substrate MP-*p*-NA. Kinetic parameters for both Co(II)- and Fe(II)-loaded WT and H178A enzymes indicate that, in general, the effect on activity is due to a decrease in k_{cat} (Table 1). K_m values were not affected for MGMM but increased moderately (~2-fold) for MP-*p*-NA. It is possible that H178A forms an hydrogen bond with either the NO_2 or the proline group of MP-*p*-NA, but at this time nothing is known about how this substrate interacts with MetAPs. The combination of these data, indicate that while H178 plays a role in the catalytic mechanism, it is not a critical residue since a significant amount of catalytic activity is retained even in its absence.

H178A *Ec*MetAP-I was found to bind only one divalent metal ion tightly, which is identical to the WT enzyme. Therefore, alteration of H178 does not affect the ability of the enzyme to bind divalent metal ions. These data are also consistent with the K_d values determined by both kinetic and ITC measurements. The K_d values determined for Fe(II) binding to WT and H178A *Ec*MetAP-I by activity titrations (0.2 vs 0.3 μM, respectively) are identical within error. On the other hand, the K_d values obtained for Co(II) binding to WT and H178A measured by ITC are similar but slightly different (6.5 vs 12.5 μM, respectively) from each other (Table 2). The small difference in Co(II) K_d values between WT and the H178A enzyme likely reflects the lack of hydrogen bond formation in the H178A enzyme. As shown in the X-ray structure of *Ec*MetAP-I, H178 forms a hydrogen bond to a water molecule, which in turn forms a hydrogen bond to the water molecule that binds to the catalytic divalent metal ion. The loss of this hydrogen bonding interaction may slightly perturb the enzymes ability to coordinate the active site divalent metal ion.

The catalytic role of H178 was further examined by recording the pH dependence of V_{max} for Co(II)-loaded WT and H178A *Ec*MetAP-I. Plots of V_{max} vs pH are bell shaped for both WT and H178A Co(II)-loaded *Ec*MetAP-I (Figure 3). In addition, both enzymes displayed optimum catalytic efficiency and maximal activity between pH values of 7.5 and 7.8 toward MGMM. However, enzyme stability studies

indicated that the H178A enzyme quickly loses activity above pH 7.5, and little if any activity could be recovered after the enzyme was incubated at pH 8.5 for the time required to perform the assay (>1 h) (Figure 3B). Therefore, no useful pK_a data could be obtained from log plots of kinetic constants vs pH at pH values above 7.8 for the H178A EcMetAP-I enzyme.

Inspection of the plot of log(K_m) vs pH for WT EcMetAP-I shows two inflections at ca. 7.5 and 7.9 where the asymptote of the sigmoidal region meets the flat, pH-independent regions. The inflection at pH 7.5 indicates that a protonated form of the substrate or a group on the enzyme results in increased substrate binding affinity assisting in ES complex formation. This p$K_a$value is assigned to the deprotonation of the N-terminal α-amino group of the substrate MGMM (pK_S). This assignment is based on the pK_a of N-terminal amine of MGMM which is 7.5 ([40]) and also upon the similarity of the observed pK_a to the pK_a of the N-terminal α-amino group of the substrate L-p-NA which is 7.74 ([41]). These data indicate that the protonated form of the substrate binds to the enzyme more tightly than the deprotonated form. At pH values below 7.4, the log(K_m) vs. pH plot of the WT enzyme does not change appreciably, while the H178A enzyme exhibits a slight decrease in K_m with increasing acidity (pH < 7.2). These data suggest a small build up of hydronium ions may occur in place of H178 which, in turn, may stabilize substrate binding. Alternatively, the lack of the imidazole may cause greater steric freedom and thus a better fit for substrate. The slight increase in K_m observed for MP-p-NA may be due to a decrease in van der Waals interactions with the cyclic portion of the proline residue of the substrate and suggests that H178A may affect the way certain substrates bind to the EcMetAP-I active site. The inflection on the basic side of the log(K_m) vs. pH plot for WT EcMetAP-I at pH 7.9 is likely due to an ionization on the enzyme since there are no other ionizable groups with reasonable pK_a's on the substrate. Protonation of this groupfacilitates better binding of the substrate as shown in Scheme 1.
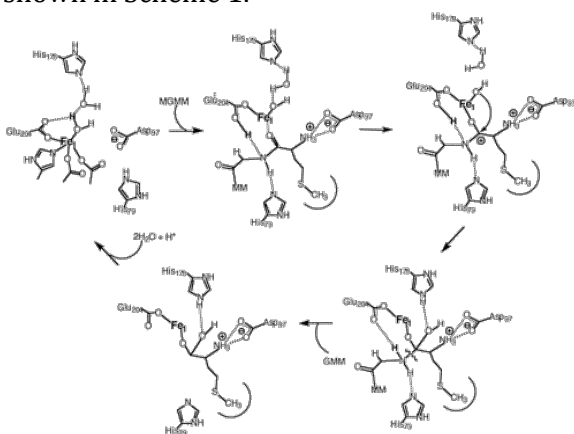

Figure 8 Proposed Catalytic Mechanism for EcMetAP-I.

A plot of log(k_{cat}) vs. pH for WT EcMetAP-I is bell-shaped, while the same plot for H178A shows increasing k_{cat} as the pH is increased up to pH 7.8. Fits of log(k_{cat}) vs pH to eq 4 provides values for pK_{ES1} of 7.2 and pK_{ES2} of 7.7 for WT EcMetAP-I where the asymptotes meet the theoretical maximum k_{cat} (k'_{cat}) (Figure 4B). These data were also fit to eq 10, which is used when the pK's are separated by less than 0.6 pH units, and provided values of pK_{ES1} = pK_{ES2}= 7.5. These data indicate that one ionizable group (pK_{ES1}) must be deprotonated while a second ionizable group must be in the protonated form (pK_{ES2}) in the ES complex for catalysis to occur. The slopes of the asymptotes calculated as prescribed ([37]) for the acidic and basic limbs of log(k_{cat}) vs. pH for WT EcMetAP-I indicate that one group is ionized on each limb. Because plots of log(k_{cat}) vs pH for both WT and H178A EcMetAP-I are identical within error, H178 is not the general base in catalysis.

Enzyme centered ionizable groups were gleaned from plots of log(k_{cat}/K_m) vs pH since it is possible to determine pKvalues centered on the free enzyme and free substrate ([36]). Similar to the plots of log(k_{cat}) vs pH for WT and H178A EcMetAP-I, plots of log(k_{cat}/K_m) vs pH are bell-shaped for both WT EcMetAP-I and H178A. Fits of log(k_{cat}/K_m) vs pH for WT EcMetAP-I to eq 5 provides two ionizations values with pK_{E1} = 7.7

and $pK_{E2} = 6.6$. Both asymptotes have slopes of ~1 indicating a single ionizable group exists at both high and low pH. The large difference between the k'_{cat}/k'_m and the apparent k_{cat}/K_m results in pK_{E1} being greater than pK_{E2}. Since the pK values are separated by less than 0.6 pH units, these data were fit to eq 11 (*39*) and yield pK values of $pK_{E1} = pK_{E2} = 7.1$. The existence of two ionizations indicates that there should be three different ionization states of the enzyme that affect catalytic efficiency (Scheme 1). Moreover, one of these ionizations may reflect proton dissociation from the substrate since pK_s is in the pH range studied. Possible active site residues in *Ec*MetAP-I that account for the enzyme-centered pK might include H79 or E204. H79 resides ~5 Å from Co1 while E204 is a ligand to Co1 and also forms an hydrogen bond to the metal bound water molecule.

Since pK_{E1} and pK_{E2} are not well separated for both WT and H178A *Ec*MetAP-I, the associated error is rather high. Therefore, an alternative method was utilized to directly measure a metal centered deprotonation. Electronic absorption spectra of Co(II)-loaded WT and H178A *Ec*MetAP-I were recorded as a function of pH between 6.0 and 9.0. Increasing the pH from 7.5 to 9.0 increases the molar absorptivity at 640 nm (λ_{max}) from 135 to 290 M^{-1} cm^{-1}, while decreasing the pH from 7.5 to 6.5 decreases the molar absorptivity from 135 to 50 $M^{-1}cm^{-1}$. The range of observed molar absorptivity values as a function of pH is consistent with the Co(II) remaining five-coordinate at all pH values studied (*42*). A plot of molar absorptivity (ε) of the λ_{max} value at 640 nm vs. pH provides a simple sigmoidal curve with an apparent pK_a value of 8.1. Since four ligating atoms are provided by enzyme amino acid groups, the fifth Co(II)-ligand must be a water molecule that is deprotonated to an hydroxide with a pK_a value around 8.1. This water/hydroxide likely functions as the nucleophile during catalytic turnover. We have also recorded the electronic absorption spectrum of H178A as a function of pH and found a pK_a value of ~7.6 based on a plot of molar absorptivity at 640 nm vs pH. Comparison of these data with those obtained for WT *Ec*MetAP-I indicates that the pK_a of the water/hydroxide bound to the Co(II) ion becomes more acidic by 0.5 pH units when H178 is altered to an Ala residue.

Combination of these data suggests that pK_{E1} (7.8), determined from the $\log(k_{cat}/K_m)$ vs pH plot, matches within error the pK_E (8.1) obtained from measurements of the pH dependent changes in UV−vis spectra of Co(II) *Ec*MetAP-I. Therefore, this pK was assigned to the ionization of the metal-bound water molecule. On the basis of X-ray crystallography, H178 forms a hydrogen bond with a water molecule that, in turn, hydrogen bonds to the water molecule that bridges between the two Co(II) ions providing a H178−H_2O−H_2O−Co(II) proton relay system (*43*). It appears that H178 indirectly stabilizes the metal-bound water molecule and helps to increase the pK_a value relative to that in the H178A mutant. This change in pK_a is critical for catalysis, since a metal-bound hydroxide would decrease the Lewis acidity of the divalent metal ion vs a metal-bound water molecule, thus reducing the ability of the carbonyl oxygen to bind to the metal ion and be activated.

On the basis of all of the kinetic, spectroscopic, and X-ray crystallographic data reported to date, an altered mechanism of action for *Ec*MetAP-I is proposed (Figure 8) (*21*). Since both *Ec*MetAP-I and *Pf*MetAP-II have been shown to be fully active with only a single divalent metal ion present and additional divalent metal ions are inhibitory, MetAPs have been reclassified, by one of us, as mononuclear metalloproteases (*23*). At the same time, the crystal structure of *Ec*MetAP-I and the close relatives including *Pf*MetAP-II, *Hs*MetAP-II, and aminopeptidase P show two metal ions in the active site (*44*). The catalytically active metal ion in *Ec*MetAP-I is coordinated by H171 (*23, 25*). On the basis of the recently proposed mechanism for the leucine aminopeptidase from *Aeromonas proteolytica* (*45*), the first step in catalysis for MetAPs is likely recognition of the N-terminal methionine side chain by the hydrophobic pocket adjacent to the metallo-active site (*21, 43*). Next, the peptide carbonyl oxygen coordinates to the histidine-ligated divalent metal ion. Hydrogen bond formation between His79 and the backbone N−H scissile peptide bond has been proposed based on X-ray crystallographic results, thereby stabilizing the leaving group (*21, 43*). In addition, Glu204, which is also a ligand to the histidine-containing divalent metal ion, was proposed to be a proton acceptor/donor in the catalytic process (*21, 43*). This assignment is consistent with the observed pK_{ES1} of 7.2 for the hydrogen bound Glu204 deprotonation process. Since the N-terminal amine nitrogen of the substrate forms a hydrogen bond with D97 based on X-ray crystallography, in the absence of a second

metal ion D97 likely assists to position the substrate properly in the active site for formation of the transition-state intermediate. This proposal is based on the fact that protonated MGMM binds more tightly to *Ec*MetAP-I as well as the crystal structure of *Ec*MetAP-I with a substrate analogue inhibitor in which the N-terminal amine nitrogen is coordinated to the second Co(II) ion and forms hydrogen bonds to D97. Assignment of pK_{E2} (7.9) to H79, based on the plot of log K_m vs pH, is likely since H79 forms a hydrogen bond to the backbone amine nitrogen of the substrate, based on X-ray crystallography. Next, the product-forming C−N bond-breaking step occurs followed by the release of the cleaved peptide. Finally, the active site adds two water molecules: one that binds to the divalent metal ion and one that bridges between the coordinated water molecule and H178. Therefore, H178 helps to regulate the pK_a of the metal bound nucleophile, but does not function as the active site general acid/base.

In summary, the new data provide support for the key elements of the previously proposed mechanism (*21*) and suggest that a similar mechanism can apply to the enzyme with a single metal ion bound in the active site.

References

1 Bradshaw, R. A. (1989) *Trends Biochem. Sci.14*, 276−279.

2 Meinnel, T., Mechulam, Y., and Blanquet, S. (1993)*Biochimie75*, 1061−1075.

3 Bradshaw, R. A., Brickey, W. W., and Walker, K. W. (1998) *Trends Biochem. Sci.23*, 263−267.

4 Arfin, S. M., and Bradshaw, R. A. (1988)*Biochemistry27*, 7979−7984.

5 Hirel, P.-H., Schmitter, J.-M., Dessen, P., Fayat, G., and Blanquet, S. (1989) *Proc. Natl. Acad. Sci. U.S.A.86*, 8247−8251.

6 Ben-Bassat, A., and Bauer, K. (1987) *Nature326*, 315.

7 Tobias, J. W., Shrader, T. E., Rocap, G., and Varshavsky, A. (1991) *Science254*, 1374−1377.

8 Chang, S.-Y. P., McGary, E. C., and Chang, S. (1989)*J. Bacteriol.171*, 4071−4072.

9 Chang, Y.-H., Teichert, U., and Smith, J. A. (1992) *J. Biol. Chem.267*, 8007−8011.

10. Li, X., and Chang, Y.-H. (1995) *Proc. Natl. Acad. Sci. U.S.A.92*, 12357−12361.

11 Miller, C. G., Kukral, A. M., Miller, J. L., and Movva, N. R. (1989) *J. Bacteriol.171*, 5215−5217.

12 Taunton, J. (1997) *Chem. Biol.4*, 493−496.

13 Griffith, E. C., Su, Z., Turk, B. E., Chen, S., Chang, Y.-H., Wu, Z., Biemann, K., and Liu, J. O. (1997) *Chem. Biol.4*, 461−471.

14 Sin, N., Meng, L., Wang, M. Q., Wen, J. J., Bornmann, W. G., and Crews, C. M. (1997) *Proc. Natl. Acad. Sci. U.S.A.94*, 6099−6103.

15 Lowther, W. T., McMillen, D. A., Orville, A. M., and Matthews, B. W. (1998) *Proc. Natl. Acad. Sci. U.S.A.95*, 12153−12157.

16 Liu, S., Widom, J., Kemp, C. W., Crews, C. M., and Clardy, J. (1998) *Science282*, 1324−1327.

17 Miller, C. G., Strauch, K. L., Kukral, A. M., Miller, J. L., Wingfield, P. T., Mazzei, G. J., Werlen, R. C., Graber, P., and Movva, N. R. (1987) *Proc. Natl. Acad. Sci. U.S.A.84*, 2718−2722.

18 Tahirov, T. H., Oki, H., Tsukihara, T., Ogasahara, K., Yutani, K., Ogata, K., Izu, Y., Tsunasawa, S., and Kato, I. (1998) *J. Mol. Biol.284*, 101−124.

19 Roderick, S. L., and Matthews, B. W. (1993)*Biochemistry32*, 3907−3912.

20. Lowther, W. T., Orville, A. M., Madden, D. T., Lim, S., Rich, D. H., and Matthews, B. W. (1999) *Biochemistry38*, 7678−7688.

21 Lowther, T. W., Zhang, Y., Sampson, P. B., Honek, J. F., and Matthews, B. W. (1999) *Biochemistry38*, 14810−14819.

22 D'souza, V. M., and Holz, R. C. (1999)*Biochemistry38*, 11079−11085.

23 D'souza, V. M., Bennett, B., Copik, A. J., and Holz, R. C. (2000) *Biochemistry39*, 3817−3826.

24 Meng, L., Ruebush, S., D'Souza V, M., Copik, A. J., Tsunasawa, S., and Holz, R. C. (2002) *Biochemistry41*, 7199−208.

25 Cosper, N. J., D'souza, V., Scott, R., and Holz, R. C. (2001) *Biochemistry40*, 13302−13309.

26 Matthews, B. W. (1988) *Acc. Chem. Res.21*, 333−340.

27 Vallee, B. L., and Auld, D. S. (1993) *Proc. Natl. Acad. Sci. U.S.A.* *90*, 2715−2718.

28 Vallee, B. L., and Galdes, A. (1984) *Adv. Enzymol.* *56*, 283−430.

29 Vallee, B. L., and Auld, D. S. (1990) *Biochemistry* *29*, 5647−5659.

30. Christianson, D. W., and Lipscomb, W. N. (1989) *Acc. Chem. Res.* *22*, 62−69.

31 Lowther, W. T., and Matthews, B. W. (2000) *Biochim. Biophys. Acta* *1477*, 157−67.

32 Zhou, Y., Gou, X.-C., Yi, T., Yoshimoto, T., and Pei, D. (2000) *Anal. Biochem.* *280*, 159−165.

33 Winzor, D. J., and Sawyer, W. H. (1995) *Quantitative Characterization of Ligand Binding*, Wiley-Liss, New York.

34 Segel, I. H. (1975) *Enzyme Kinetics: Behavior and Analysis of Rapid Equilibrium and Steady-State Enzyme Systems*, 1st ed., John Wiley & Sons, New York.

35 Cornish-Bowden, A. (1995) *Fundamentals of Enzyme Kinetics*, Portland Press Ltd., London.

36 Dixon, M., and Webb, E. C. (1979) *Enzymes*, 3rd ed., Academic Press, New York.

37 Cleland, W. W. (1997) *Adv. Enzymol. Relat. Areas Mol. Biol.* *45*, 273−387.

38 Tipton, K. F., and Dixon, H. B. (1997) *Methods Enzymol.* *63*, 183−234.

39 Cleland, W. W. (2003), personal communication.

40. Strzelczak, G., Bobrowski, K., and Holcman, J. (1998) *Radiat. Res.* *150*, 688−694.

41 Baker, J. O., and Prescott, J. M. (1983) *Biochemistry* *22*, 5322−5331.

42 Bertini, I., and Luchinat, C. (1984) in *Adv. Inorg. Biochem.* (Eichhorn, G. L., and Marzilli, L. G., Eds.) pp 71−111, Elsevier, New York.

43 Lowther, W. T., Orville, A. M., Madden, D. T., Lim, S., Rich, D. H., and Matthews, B. W. (1999) *Biochemistry* *38*, 7678−7688.

44 Lowther, W. T., and Matthews, B. W. (2000) *Biochim. Biophys. Acta* *1477*, 157−167.

45 Ustynyuk, L., Bennett, B., Edwards, T., and Holz, R. C. (1999) *Biochemistry* *38*, 11433−11439.

1 Abbreviations: *Ec*MetAP-I (methionyl aminopeptidase from *E. coli*); *Pf*MetAP-II (methionyl aminopeptidase from *Pyrococcus furiosus*); *Hs*MetAP-II (human methionyl aminopeptidase); HEPES ([4-(2-hydroxyethyl)-1-piperazineethanesulfonic acid]); MES ([2-(*N*-morpholino)ethanesulfonic acid]); EPPS (*N*-2-hydroxyethylpiperazinepropane sulfonic acid); Tricine (*N*-tris[hydroxymethyl]methylglycine; ICP-AES (inductively coupled plasma-atomic emission spectroscopy); AAP (aminopeptidase from *Aeromonas proteolytica*); blLAP (bovine lens leucine aminopeptidase); WT (wild-type); ITC (isothermal titration calorimetry); MGMM (Met−Gly−Met−Met); MP-*p*-NA (Met-Pro-*p*-nitroanilide); Nle-AAEE (norleucine−Ala−Ala−Glu−Glu).